AAS 10-032

DEMONSTRATION OF AN AEROCAPTURE GN&C SYSTEM THROUGH HARDWARE-IN-THE-LOOP SIMULATIONS

James Masciarelli,[*] Jennifer Deppen,[†] Jeff Bladt[‡], Jeff Fleck[§], Dave Lawson[**]

Aerocapture is an orbit insertion maneuver in which a spacecraft flies through a planetary atmosphere one time using drag force to decelerate and effect a hyperbolic to elliptical orbit change. Aerocapture employs a feedback Guidance, Navigation, and Control (GN&C) system to deliver the spacecraft into a precise post-atmospheric orbit despite the uncertainties inherent in planetary atmosphere knowledge, entry targeting and aerodynamic predictions. Only small amounts of propellant are required for attitude control and orbit adjustments, thereby providing mass savings of hundreds to thousands of kilograms over conventional all-propulsive techniques. The Analytic Predictor Corrector (APC) guidance algorithm has been developed to steer the vehicle through the aerocapture maneuver using bank angle control.. Through funding provided by NASA's In-Space Propulsion Technology Program, the operation of an aerocapture GN&C system has been demonstrated in high-fidelity simulations that include real-time hardware in the loop, thus increasing the Technology Readiness Level (TRL) of aerocapture GN&C. First, a non-real-time (NRT), 6-DOF trajectory simulation was developed for the aerocapture trajectory. The simulation included vehicle dynamics, gravity model, atmosphere model, aerodynamics model, inertial measurement unit (IMU) model, attitude control thruster torque models, and GN&C algorithms (including the APC aerocapture guidance). The simulation used the vehicle and mission parameters from the ST-9 mission. A 2000 case Monte Carlo simulation was performed and results show an aerocapture success rate of >99.7%, >95% of total delta-V required for orbit insertion is provided by aerodynamic drag, and post-aerocapture orbit plane wedge angle error is <0.5 deg (3-sigma). Then a real-time (RT), 6-DOF simulation for the aerocapture trajectory was developed which demonstrated the guidance software executing on a flight-like computer, interfacing with a simulated IMU and simulated thrusters, with vehicle dynamics provided by an external simulator. Five cases from the NRT simulations were run in the RT simulation environment. The results compare well to those of the NRT simulation thus verifying the RT simulation configuration. The results of the above described simulations show the aerocapture maneuver using the APC algorithm can be accomplished reliably and the algorithm is now at TRL-6. Flight validation is the next step for aerocapture technology development.

[*] Principal Investigation, Ball Aerospace & Technologies Corp., 1600 Commerce St., Boulder, CO.
[†] Systems/Project Engineer, Ball Aerospace & Technologies Corp., 1600 Commerce St., Boulder, CO.
[‡] ADCS Engineer, Ball Aerospace & Technologies Corp., 1600 Commerce St., Boulder, CO.
[§] Flight Software Engineer, Ball Aerospace & Technologies Corp., 1600 Commerce St., Boulder, CO
[**] Real Time Simulator Lead, Ball Aerospace & Technologies Corp., 1600 Commerce St., Boulder, CO

INTRODUCTION

Aerocapture is an orbit insertion maneuver in which a spacecraft flies through a planetary atmosphere one time using drag force to decelerate and effect a hyperbolic to elliptical orbit change. This is in contrast to the related technique of multi-pass aerobraking which uses drag to circularize the orbit of an already captured spacecraft. By using aerocapture, propellant mass is significantly reduced, which allows delivery of more scientific payload to the planet, or use of a smaller launch vehicles for Earth departure. This in turn, enables more extensive and cost effective space science missions. Aerocapture employs a feedback Guidance, Navigation, and Control (GN&C) system to deliver the spacecraft into a precise post-atmospheric orbit despite the uncertainties inherent in planetary atmosphere knowledge, entry targeting and aerodynamic predictions. Only small amounts of propellant are required for attitude control and orbit adjustments, thereby providing mass savings of hundreds to thousands of kilograms over conventional all-propulsive techniques.

A key element required for aerocapture is the GN&C system that steers the vehicle through the atmosphere and delivers it into a precise orbit. The Analytic Predictor Corrector (APC) guidance algorithm has been developed to steer the vehicle through the aerocapture maneuver using bank angle control. The algorithm is derived from that developed for the Aeroassist Flight Experiment (AFE) program circa 1989 and has been refined through several aerocapture systems analysis studies for aerocapture at Mars, Titan, Neptune, Venus, and Earth.[1] These efforts have resulted in a mature, flexible, and robust algorithm that is independent of vehicle and mission design parameters, tolerates dispersions and uncertainties in atmosphere density, vehicle mass, aerodynamics, and delivery and knowledge errors. The APC algorithm has shown excellent performance in ground-based simulations of missions to Earth, Titan, Mars, Venus, and Neptune. Three sigma (99.87%) success rates or better have been shown for all destinations using conservative models for atmospheric density profile uncertainty, approach navigation errors, and vehicle aerodynamic property uncertainties. Details of the guidance development and testing efforts can be found in a series of previously published papers.[2 3 4 5 6 7 8 9 10 11 12]

Ball Aerospace was competitively selected through a NASA Research Announcement process to provide the APC guidance algorithm and software for NASA's New Millennium Program ST9 mission. Ball Aerospace developed a complete prototype implementation of the APC guidance algorithm, completed initial six degree-of-freedom (6-DOF) aerocapture trajectory simulations with NASA, and was to provide a flight software implementation of the algorithm and perform testing and flight validation on the ST9 mission. The ST9 Aerocapture Mission completed a year-long Concept Definition Phase, but was not selected for further implementation. However, in order to continue maturing aerocapture technology, NASA's In-Space Propulsion Technology Office is continuing the guidance algorithm development work that was to take place under the ST9 mission. Ball Aerospace has leveraged the prior work, along with our existing flight software development and test benches from other programs, to further mature this aerocapture technology.

MISSION OVERVIEW

Aerocapture Trajectory Overview

An aerocapture trajectory consists of the following main events (as illustrated in Figure 1):

- Entry Targeting – The vehicle approaches the target planet and the trajectory is adjusted such that the atmospheric entry angle is within acceptable bounds.
- Atmospheric Entry – The vehicle enters the atmosphere and begins to decelerate due to aerodynamic drag.

- Energy Dissipation – The vehicle flies through the atmosphere at nearly constant altitude to dissipate excess energy.
- Controlled Atmosphere Exit – Once sufficient energy has been dissipated, the vehicle flies out of the atmosphere, controlling the altitude rate and velocity at atmospheric exit so as to achieve the target orbit apoapsis.
- Exit Atmosphere – The vehicle leaves the atmosphere and deceleration due to aerodynamic drag is nearly zero.
- Periapsis Raise – After coasting to the orbit apoapsis altitude, a small propulsive maneuver is used to raise periapsis to the desired altitude so that the vehicle does not reenter the atmosphere.

For this project, the phases from Atmospheric Entry to Atmospheric Exit were simulated and tested.

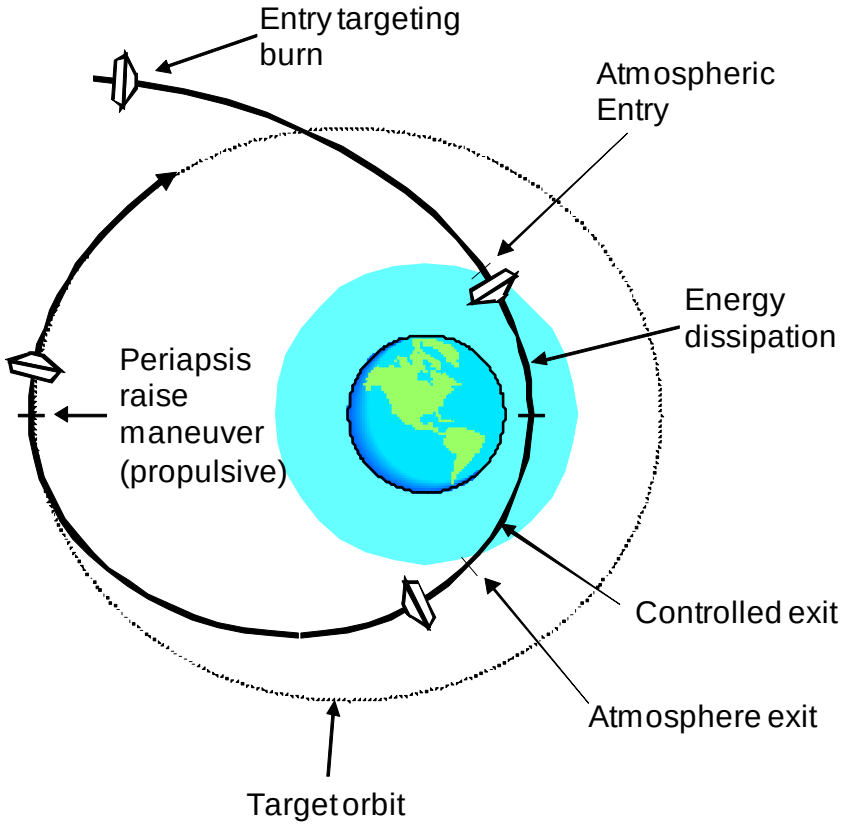

Figure 1. Key events in an aerocapture trajectory.

Analytic Predictor-Corrector Algorithm

A key component required to perform aerocapture is the guidance algorithm, which generates commands to steer the vehicle through the atmosphere to the desired final apoapsis altitude and inclination. The Analytic Predictor-Corrector (APC) aerocapture guidance algorithm guides a lifting vehicle through the atmosphere to a desired exit condition (based on the desired apoapsis

altitude and inclination) by commanding rotation about the vehicle's velocity vector (bank angle) as shown in Figure 2. During atmospheric flight, the vehicle's aerodynamic drag provides the change in velocity needed to capture into orbit, while aerodynamic lift provides the capability to control the trajectory under dispersions. The guidance algorithm continuously computes bank angle (rotation about the velocity vector as shown in Figure 2) commands to point the lift vector in the desired direction and steer the trajectory under dispersions. The vehicle's control system receives the steering commands from the guidance and fires the vehicle's attitude control thrusters to rotate the vehicle about the velocity vector, and achieve the commanded bank angle.

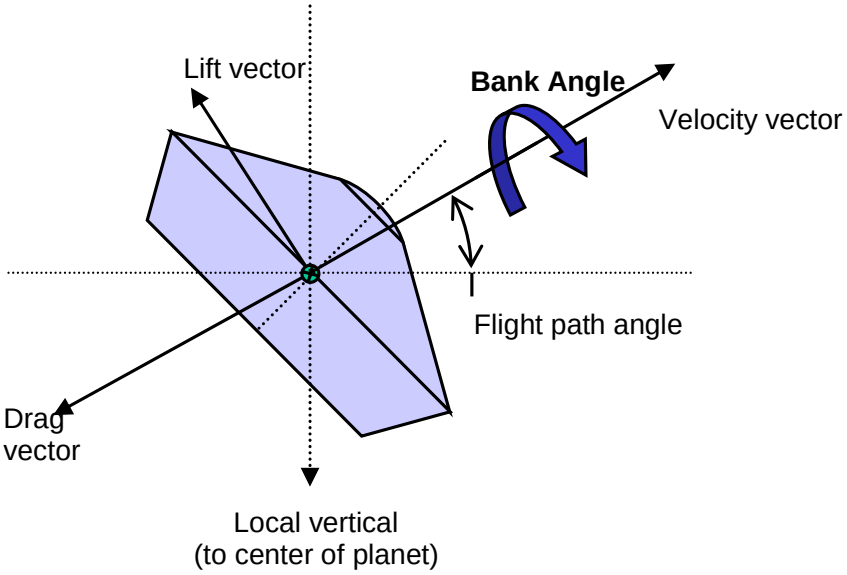

Figure 2. The aerocapture trajectory is controlled through bank angle modulation, which is rotation about the velocity vector.

The top-level logic flow of the guidance algorithm is shown in Figure 3. By design, the algorithm uses a sequence of non-iterative, non-recursive calculations that result in a very efficient, predictable, and consistent execution time. Inputs to the guidance algorithm are the current vehicle position vector, velocity vector, sensed acceleration vector, and vehicle attitude; all obtained from the on-board navigation system. When the vehicle is outside of the atmosphere, it commands the bank angle based on its estimated position in the entry corridor. Once inside the atmosphere, the algorithm uses the sensed acceleration to estimate the atmospheric density and adjusts the predicted density profile by scaling its internal density model. Drag and altitude rate error are then used to compute the bank angle magnitude that results in the desired apoapsis altitude. Bank angle direction is selected to steer toward the desired orbit plane. The algorithm outputs a desired bank angle and direction to rotate (clockwise or counter clockwise), which is executed by the vehicle's attitude control system. Some of the features of the APC algorithm are listed in Table 1.

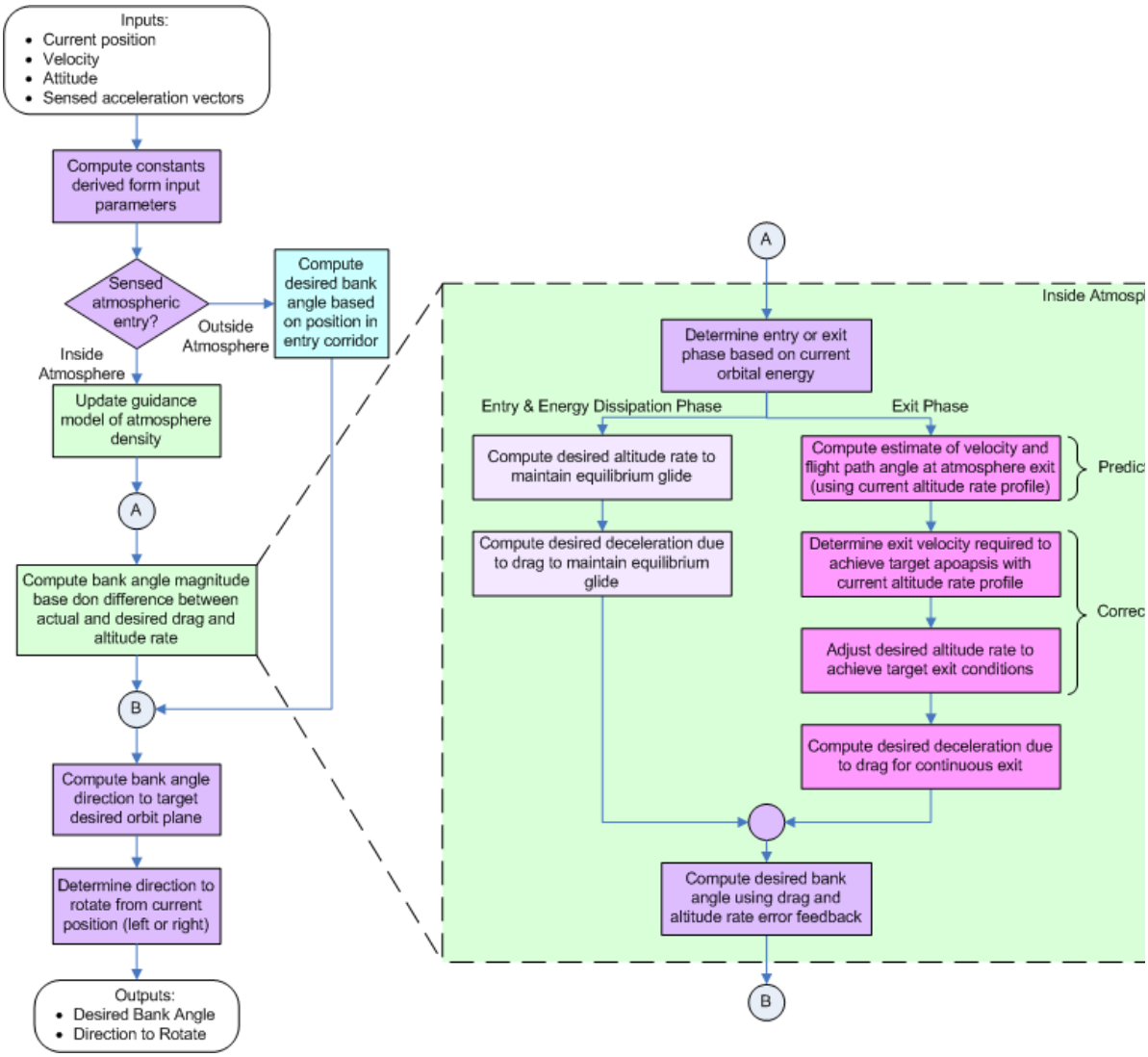

Figure 3. Guidance algorithm logic is sequential and non-recursive, with separately controlled entry and exit phases.

Table 1. APC Algorithm Features.

Feature	Algorithm Design
Tolerance to atmosphere density uncertainty, variability, and random perturbations	Sensed acceleration vector used to estimate density bias and scale height. Using a density filter, the on-board model of the atmosphere density is updated to accurately reflect the actual atmosphere.
Tolerance to variability in L/D	Sensed acceleration vector used to estimate L/D during flight and adjust bank angle command, compensating for sensitivity to L/D variability.
Tolerance to variability in ballistic coefficient	Variation in ballistic coefficient results in bias in measured density, which is automatically compensated for by density estimation filter.
Tolerance to variability in trim angle of attack	Variability in angle of attack results in variability in L/D and ballistic coefficient, which are handled as discussed above.
Tolerance to entry flight path angle delivery errors	Bank command before entry computed from estimated position in entry corridor. Algorithm captures nearly 100% of theoretical entry corridor.
Tolerance to IMU errors (altitude rate knowledge error)	Use of desired deceleration due to drag that is independent of altitude rate as a feedback control variable.
CPU load / execution time	Short, non-iterative sequence of computations provides fast, consistent execution time.
Orbit altitude targeting	Generalized exit predictor logic enables flexibility in accurately targeting a large range of orbit altitudes.
Orbit plane targeting	Determining bank reversal direction using desired deceleration due to drag and altitude rate minimizes orbit plane error while maintaining orbit altitude targeting accuracy.
Flexibility	Variable duration of guidance phases fits wide range of mission parameters. Only 40 initialization parameters required to adjust to different mission conditions.
Extensibility	Guidance designed with separate, modular phases, with possible addition of new phases without affecting other phases. Angle-of-attack modulation can be incorporated with one new line of code.

Reference Mission Description

The ST9 Earth aerocapture mission was selected for the simulations in this project.[13] The ST9 mission planned to use a three-axis controlled spacecraft that consists of a conventional spacecraft bus located inside a blunt body aeroshell that simultaneously provides aerodynamic forces (lift and drag) and protects the spacecraft from the heating and pressure loads experienced during hypersonic flight.

The vehicle parameters assumed for the simulations were:

- Lift-to-Drag ratio (L/D) = 0.20
- Ballistic coefficient (m/CDA) = 209 kg/m^2

Initial conditions for the simulation assumed an altitude of 125 km and an entry velocity of 9.9 km/s. The target orbit for the ST9 mission was 300 x 130 km with a 39.5 degree inclination. For an all-propulsive orbit insertion, the delta-V required is 2131 m/s. So in order to meet the success criteria of providing 95% of the required delta-V with the aerocapture maneuver, the delta-V required for the periapsis raise burn had to be less than 107 m/s.

NON-REAL TIME SIMULATION

A non-real-time (NRT), 6-degree-of-freedom simulation was developed to assess performance of the aerocapture algorithm in a high-fidelity environment. Both nominal and Monte Carlo trajectory simulations were completed using the NRT simulation. This section discusses the simulation and the results obtained with the simulation. The results of the NRT simulation are later compared to results obtained with the real-time, hardware in the loop simulations.

Simulation Models

In order to meet the objectives of providing a complete environment for testing the guidance algorithm, the simulation was required to include a gravity model, atmosphere model, aerodynamics model, inertial measurement unit (IMU) model, attitude control thruster torque models, and GN&C algorithms. These key models are summarized in the following subsections.

Gravity Model: The NRT simulation's gravity model is a 13 x 13 geopotential model. It is integral to the vehicle dynamics module of the simulation truth model as well as the orbit propagation module in the navigation filter.

Atmosphere Model: The atmosphere model used in the simulation is the Earth GRAM 2007.[14] This is an engineering model that provides atmosphere parameters (density, pressure, temperature) versus altitude, latitude, longitude, and season. The model not only provides nominal atmospheric values, but also simulates variability and random perturbations for Monte Carlo trajectory analysis. This includes uncertainties in current estimates, as well as perturbations based on models of dynamic processes in the atmosphere.

Aerodynamics Model: The aerodynamics model used in the simulation is version 6 of the Genesis capsule code provided by NASA. The model is based on blended data from multiple scale tests of the Genesis capsule in different flight regimes. The model produces aerodynamic coefficients (axial force, normal force, yaw moment, pitch moment, roll moment, dynamic pitch derivative, and dynamic yaw derivative) based on input of the Mach number, Knudsen number, angle of attack, and sideslip angle.

IMU Model: The inertial measurement unit model is a high-fidelity model of the Scalable Space Inertial Reference Unit (SSIRU). It includes four gyroscopes with input axis alignment relative to the spacecraft body reference frame, scale factor, rate bias, least significant bit (LSB) quantization, and register roll-over. Additionally, the model includes four accelerometers with input axis alignment relative to the spacecraft body reference frame, LSB quantization, and register roll-over.

Navigation Filter: The navigation filter is a combination of BATC heritage flight control algorithms. The attitude estimation algorithm employs a fixed-gain Kalman filter to blend star tracker and gyro measurements. For the purposes of this simulation, the star tracker measurements are not included in the attitude solution, and so attitude is propagated using gyro incremental angle measurements. As mentioned in a previous section, the orbit determination module includes a 13 x 13 geopotential gravity model.

Controller Algorithm: The attitude controller is a derivative of heritage BATC flight control algorithms. It includes a desired attitude state module, an error determination module, and proportional-integral-derivative compensator stage (with integrator stage inactive) mapping attitude error

into commanded control torque. Desired bank angle and bank direction is generated by the APC guidance law. The Desired angle of attack is computed from an on-board estimate of the Knudsen number, and the desired side-slip angle is zero. A control deadband exists on the angle of attack error and sideslip angle error to accommodate off-nominal trim conditions and minimize chatter, thereby reducing propellant consumption.

Thruster Control: Attitude control is provided via eight thrusters, configured per the ST9 aerocapture vehicle design. A set of four thrusters provides roll control and a second set of four provides pitch and yaw control. Thruster firing control employs the heritage BATC flight control algorithm, which determines a commanded on-time for each of the eight thrusters. Thruster control logic calculates thruster duty cycles required to achieve the commanded attitude control torque.

Guidance Algorithm: The APC guidance algorithm is included in the simulation. The algorithm receives its inputs from the navigation filter, then computes and sends the desired bank angle and direction of rotation to the controller algorithm.

NOMINAL TRAJECTORY RESULTS

As stated previously, the ST9 Earth aerocapture mission was used for the simulations. Before any Monte Carlo analysis was performed, a nominal case was run to verify the operation of the simulation. No perturbations were introduced for this case.

Figure 4 shows the vehicle's state (altitude, inertial velocity, inertial flight path angle, bank angle, angle of attack, and side slip angle) as a function of time for the nominal trajectory. Altitude, heating rate, deceleration (g-load), and dynamic pressure are shown as a function of inertial velocity in Figure 5 and as a function of time in Figure 6.

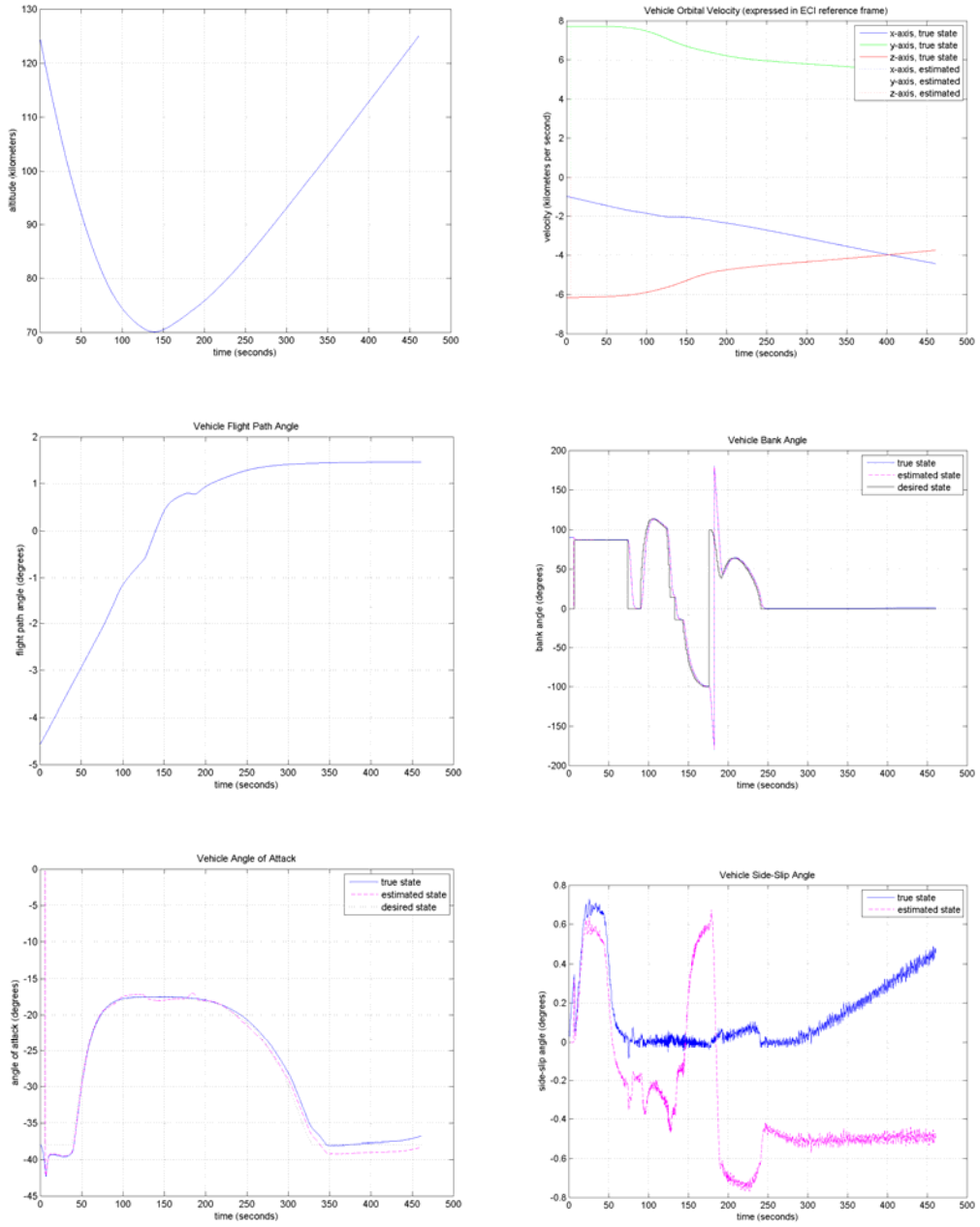

Figure 4. Nominal trajectory vehicle state (altitude, velocity, flight path angle, bank angle, angle of attack, side-slip angle) versus time.

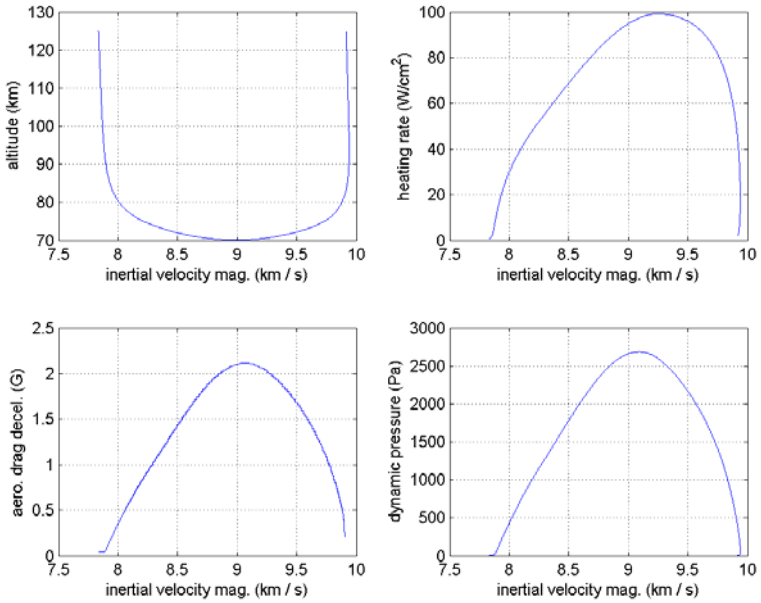

Figure 5. Altitude, heating, deceleration, and dynamic pressure versus vehicle inertial velocity magnitude for the nominal trajectory.

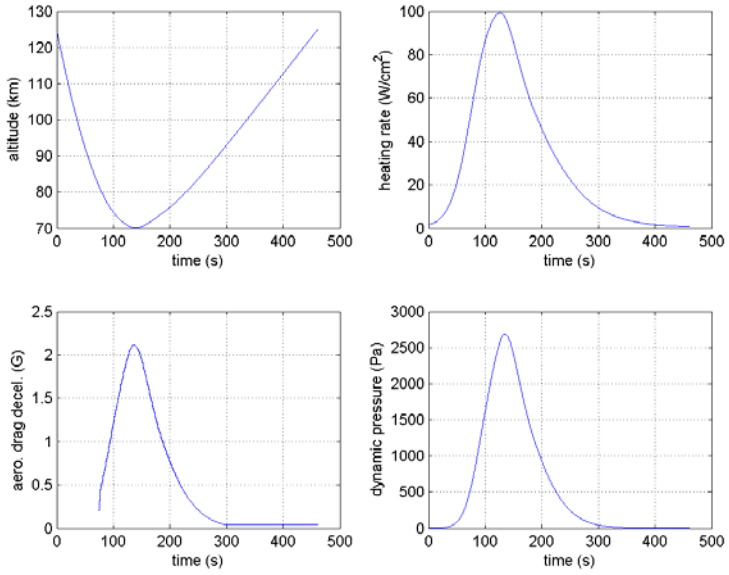

Figure 6. Altitude, heating, deceleration, and dynamic pressure versus time for the nominal trajectory.

Figure 7 demonstrates the performance of the guidance algorithm working with the navigation filter, controller, and thruster selection and pulse width logic. All of the GN&C algorithms are working as expected to successfully complete the aerocapture trajectory.

Figure 8 shows the thruster torques computed by the controller and thruster logic, which are imparted on the vehicle to produce the nominal trajectory. Figure 9 shows the resulting propellant consumption for this attitude control. As can be seen, the controller and thruster logic are operating very efficiently, using a minimum amount of propellant.

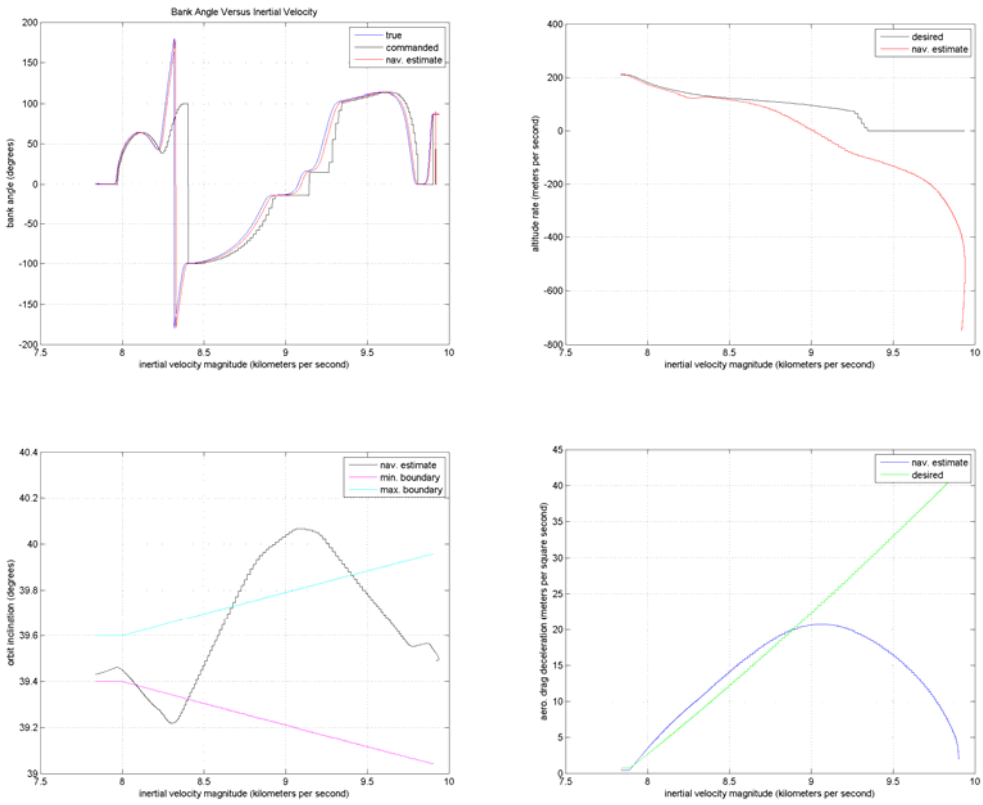

Figure 7. Desired bank angle, altitude rate, deceleration due to drag, and orbit inclination computed by the guidance algorithm compared to state in the simulation.

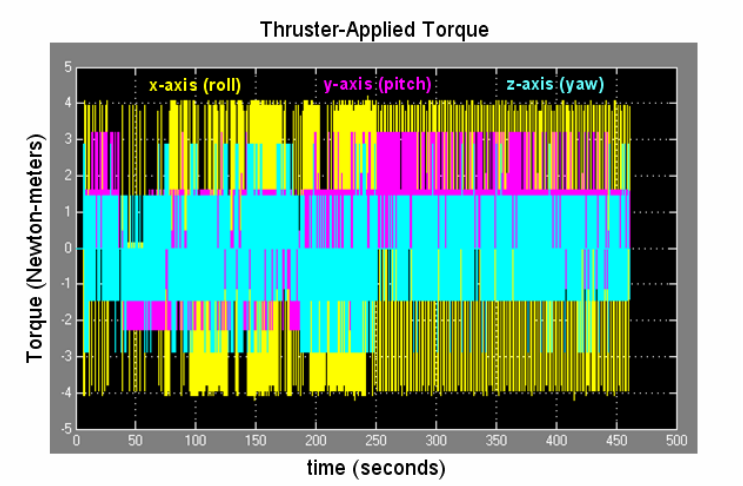

Figure 8. The controller thruster firing logic successfully controls the vehicle's attitude through the aerocapture trajectory.

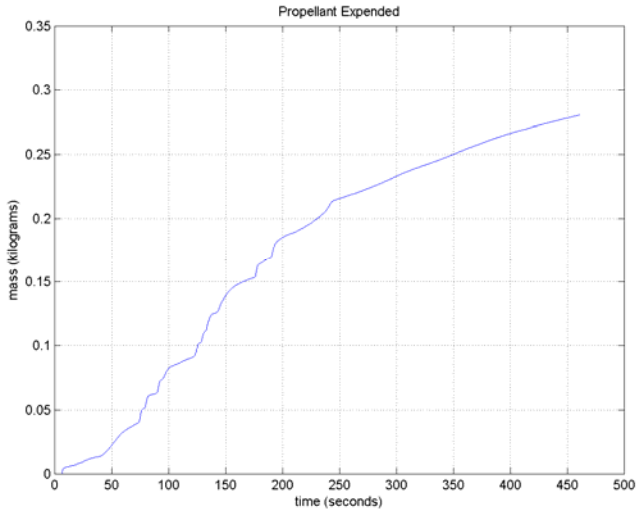

Figure 9. Cumulative propellant consumption for attitude control during the nominal aerocapture trajectory.

MONTE CARLO RESULTS

The NRT simulation was used to perform Monte Carlo trajectory simulations and determine aerocapture trajectory performance under perturbations. The following performance requirements were established to measure success:

- Aerocapture success rate of 99.7% or higher (i.e., less than 0.3% of cases in Monte Carlo analysis crash into the planet or escape from the planet).

- Targeting accuracy (3-sigma) shows that 95% or more of total delta-V required for orbit insertion is provided by aerodynamic drag.
- Post-aerocapture orbit plane wedge angle error is less than or equal to 0.5 deg (3-sigma).

A 2000 case Monte Carlo simulation was performed using the input parameters listed in Table 2. The results and statistics for the 2000 perturbed trajectories are shown in Figure 10 and Table 3. The statistics from the Monte Carlo trajectory analysis are compared against the success criteria in Table 4. As can be seen, all success criteria are satisfied.

Table 2. Monte Carlo perturbation parameters.

Input Variable	Nominal Value	Dispersion / Uncertainty
Initial Flight Path Angle	-4.537 degrees	± 0.20 degrees (3σ)
Axial aerodynamic force coefficient	aerodynamics model	± 0.1 (3σ)
Normal aerodynamic force coefficient	aerodynamics model	± 0.08 (3σ)
Side aerodynamic force coefficient	aerodynamics model	± 0.08 (3σ)
Pitch axis aerodynamic moment coefficient	aerodynamics model	± 0.12 (3σ)
Yaw axis aerodynamic moment coefficient	aerodynamics model	± 0.12 (3σ)
Pitch axis aerodynamic stability moment coefficient	aerodynamics model	± 0.28 (3σ)
Yaw axis aerodynamic stability moment coefficient	aerodynamics model	±0.28 (3σ)
Vehicle mass	198.0 kilograms	±1.0 kilogram (3σ)
Axial center of gravity location (from aft end)	0.2746 meters	0.0
Radial center of gravity location (along –z-axis)	0.0528 meters	0.0
Atmosphere	EarthGRAM 2007	variations in density, pressure, and temperature as well as random perturbations

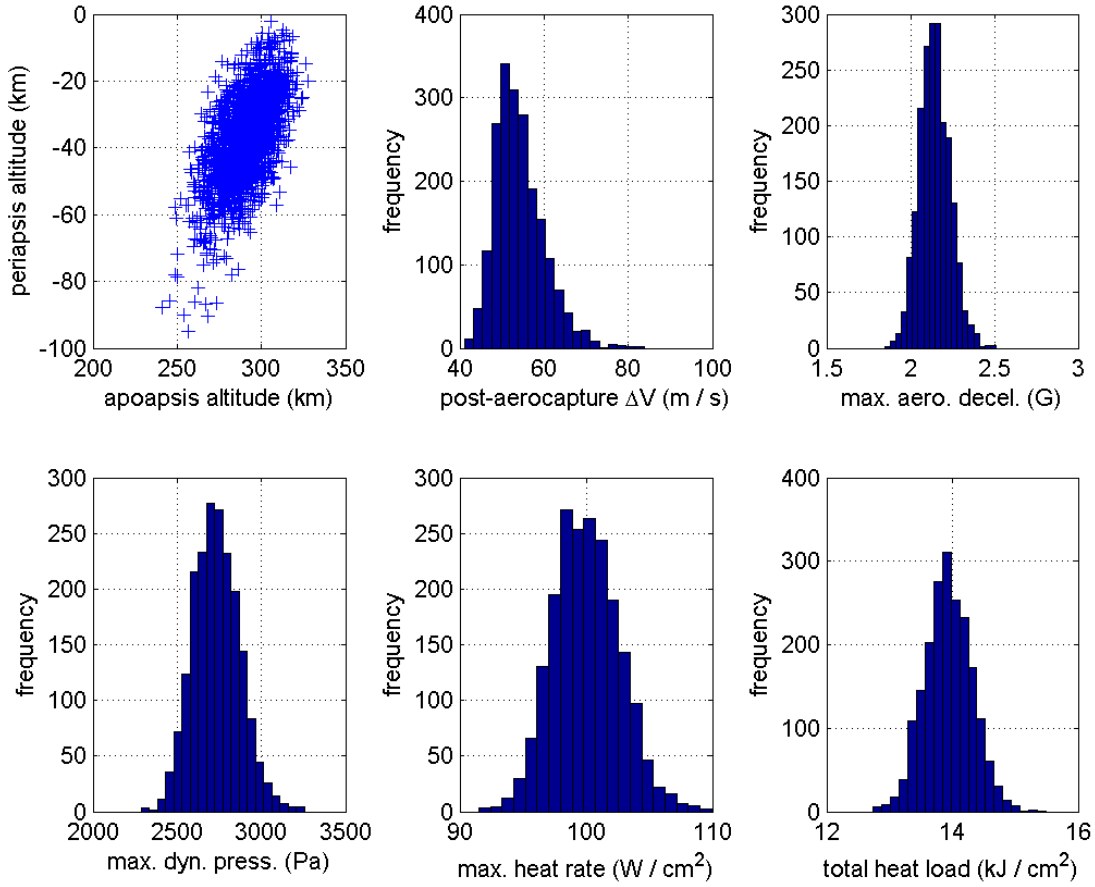

Figure 10. Results from 2000-case Monte Carlo trajectory analysis.

Table 3. Statistics from the 2000-case Monte Carlo trajectory analysis.

Parameter	Min.	Mean	Max.	Std. Deviation
Apoapsis altitude (km)	241.16	291.17	327.55	12.5
Periapsis altitude (km)	-94.82	-36.85	-1.977	12.5
Orbit plane delta-V (m/s)	41.17	54.16	83.76	5.79
Oribt inclination (deg)	39.3	39.5	39.6	0.0598
Max. drag deceleration (G)	1.85	2.14	2.51	0.091
Max. Dyn. Pressure (Pa)	2286.8	2733.7	3257.4	138.6
Max Heat Rate (W/cm2)	91.5	100.0	109.9	2.6
Total Head Load (kJ/cm2)	12.73	13.93	15.49	0.38
Total propellant mass (kg)	0.244	0.347	0.890	0.0751

Table 4. Aerocapture performance compared against success criteria.

Criteria	Requirement	Performance
Aerocapture success rate	> 99.7%	100%
Percentage of orbit insertion delta-V provided by drag	> 95% (3σ)	96.1%, worst case
Orbit Plane Wedge Angle Error	< 0.5 degree (3σ)	0.18 degree (3σ)

REAL TIME SIMULATION

The final part of the project was to develop a real time (RT) simulation to assess the performance of the APC algorithm, executing in flight software (FSW), on a flight-like computer. A nominal trajectory simulation and a subset of the Monte Carlo simulations were completed using the RT simulation and then compared to the NRT simulation results.

The real-time simulation was developed to meet the following requirements in order to provide a flight-quality, hardware-in-the-loop, simulation of the APC algorithm:

- Develop a real-time, 6-DOF simulation for the Aerocapture trajectory.
- Include at a minimum vehicle dynamics, gravity model, atmosphere model, aerodynamics model, IMU model, attitude control thruster torque models, and GN&C algorithms (including the APC Aerocapture guidance).
- Use the vehicle and mission parameters from the selected reference Aerocapture mission.
- Include hardware representative of that which could be used on a robotic class interplanetary spacecraft.
- At a minimum, demonstrate the guidance software executing on a flight-like computer, interfacing with a simulated IMU and simulated thrusters, with vehicle dynamics provided by an external simulator.
- Develop and document simulation results for the reference Aerocapture mission to demonstrate the real-time performance of the Aerocapture guidance software.

The RT simulation was assembled using engineering model avionics hardware from previous BATC programs. The hardware is coupled to a 6-DOF dynamics simulation, which not only simulates the environment, but also the inputs and outputs between the avionics and the rest of the spacecraft. The flight software running on the avionics was created by taking a flight software build from a previous BATC spacecraft program, and replacing the GN&C module with the aerocapture GN&C code. This hardware-in-the-loop, RT testbed was then used to generate aerocapture trajectory results. The results were then compared to those from the NRT simulation.

Figure 11 compares the nominal trajectory results obtained with the RT simulation with those from the NRT simulation. (See Table 4, which defines the different curves in the figures.) The results show good comparison between the NRT simulation and the RT simulation, thereby verifying the APC algorithm was correctly implemented in FSW.

In addition to the nominal case, 5 cases were chosen from the NRT Monte Carlo simulation to be simulated on the RT testbed. The results from the RT simulation were compared to the NRT simulation and showed good correlation, further verifying the algorithm has been correctly implemented in FSW and meets requirements.

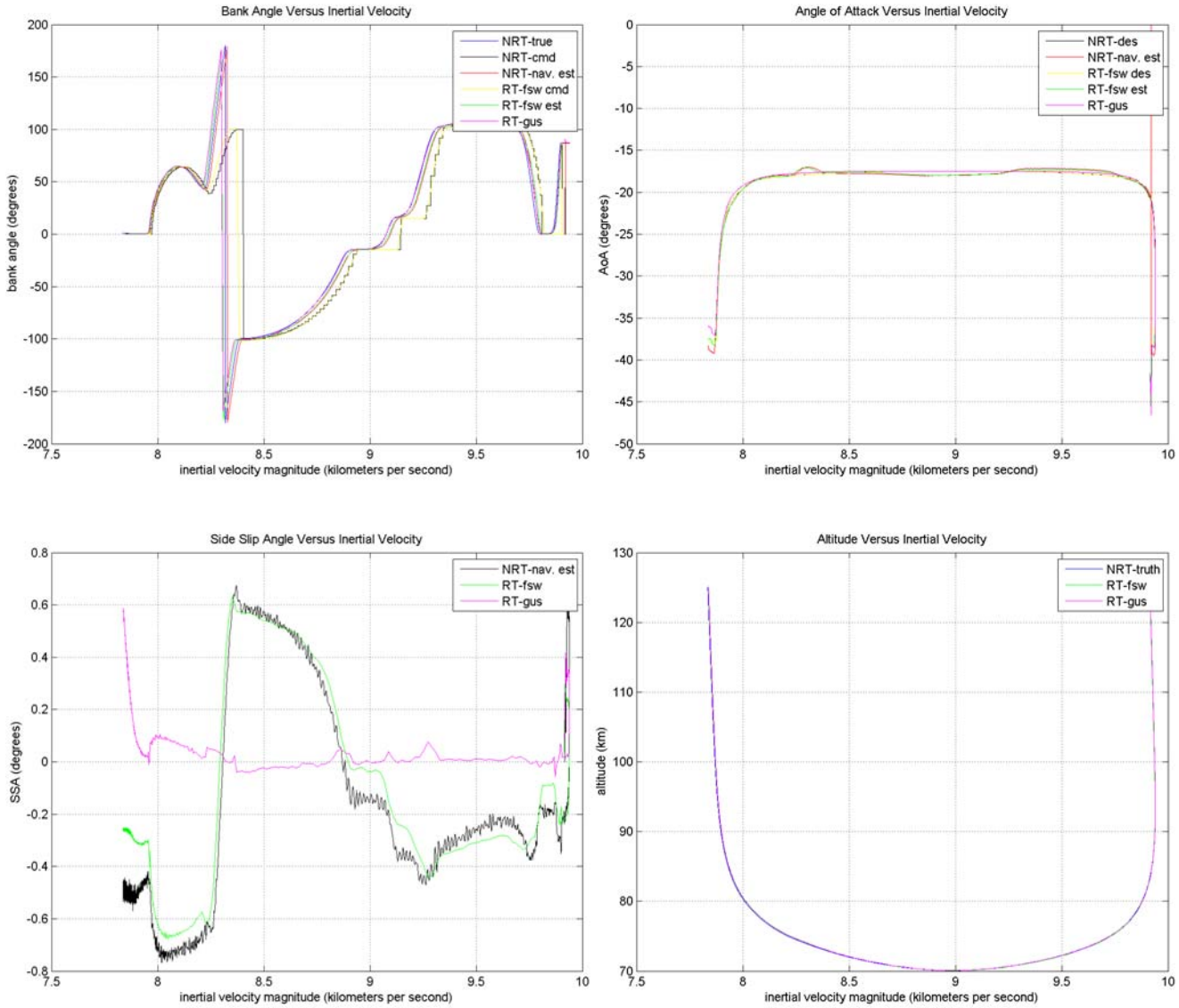

Figure 11. Comparison of RT and NRT simulation results for nominal trajectory vehicle state versus inertial magnitude.

Table 5. RT Simulation coplot legend definitions.

Plot Legend Name	Description
NRT-true	NRT simulation dynamics truth model
NRT-cmd	NRT simulation command (from guidance algorithm)
NRT-des	NRT simulation desired (from control algorithm)
NRT-nav est	NRT simulation estimate (from navigation filter)
RT-fsw cmd	RT simulation FSW command (from guidance algorithm)
RT-fsw est	RT simulation FSW estimate (from navigation filter)
RT-fsw des	RT simulation FSW desired (from control law)
RT-gus	RT simulation dynamics truth model

CONCLUSION

The overall goal of this project was to advance the TRL of the APC guidance algorithm for aerocapture through development and testing of the guidance software in real-time simulations with hardware in the loop. The data presented herein demonstrates the APC algorithm has been successfully incorporated in FSW, running on a flight-like computer, and meets all performance requirements. With the above accomplishments, all objectives of the project have been met, resulting in successful advancement of the guidance algorithm to TRL 6 as shown in Figure 12.

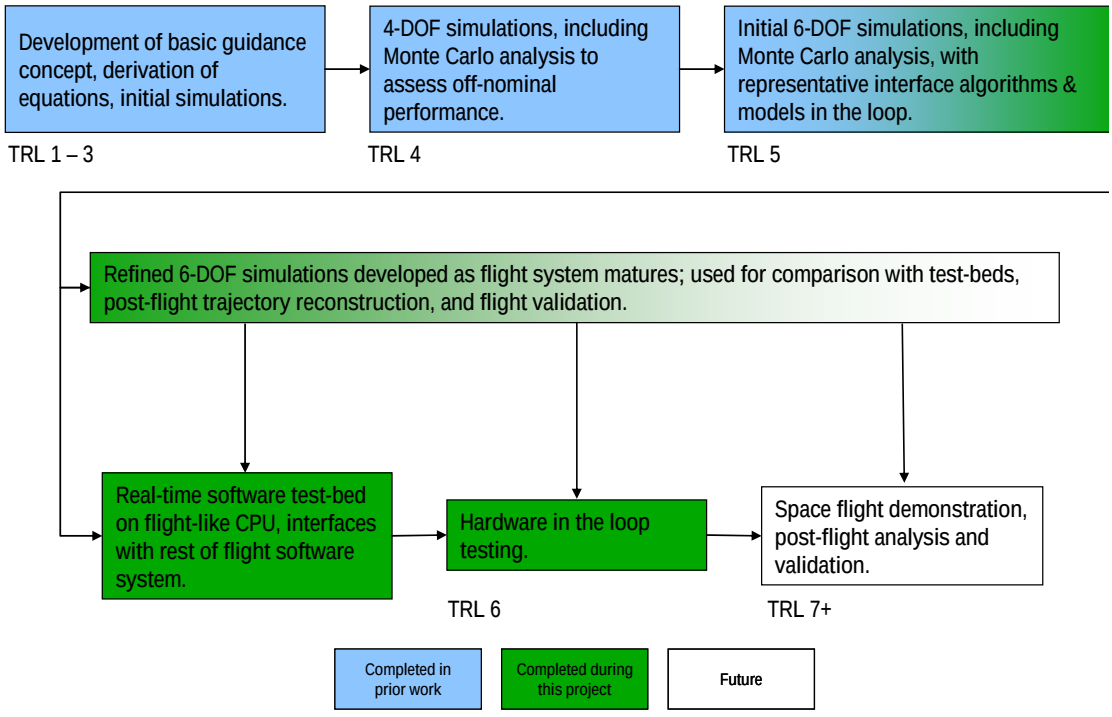

Figure 12. The APC algorithm for Aerocapture has been successfully advanced to TRL 6 as a result of this project.

ACKNOWLEDGMENTS

The work described in this paper was funded in part by the In-Space Propulsion Technologies Program, managed by NASA's Science Mission Directorate in Washington, D.C., and implemented by the In-Space Propulsion Technology Projects Office at Glenn Research Center. The authors wish to acknowledge the valuable discussions and contributions from Michelle Munk and Eric Queen from NASA Langley.

REFERENCES

[1] Bragg, B.; Cerimele, C.; Delventhal, R.; Gamble, J.; Hill, O.; Kincade, R.; Lee, D.; Long, W., McHenry, R.; McSwain, G.; Nagy, K.; Richardson, M.; Ried, R.; Roberts, B.; Scott, C.; Smith, D.; "A Design Study for an Aeroassist Flight Experiment," NASA Johnson Space Center, JSC-20593, June 1985.

[2] Gamble, J.D.; Cerimele, C.J.; Moore, T.E.; Higgins, J.; "Atmospheric Guidance Concepts for an Aeroassist Flight Experiment," The Journal of the Astronautical Sciences, Vol. 36, Nos. 1/2, January-June 1988, pp. 45-71

[3] Bryant, L.; Tigges, M.; Ives, D.; "Analytic Drag Control for Precision Landing and Aerocapture," AIAA-98-4572, AIAA Atmospheric Flight Mechanics Conference, Boston, MA, Aug. 1998.

[4] Masciarelli, J.; Rousseau, S.; Fraysse, H.; Perot, E.; "An Analytic Aerocapture Guidance Algorithm for the Mars Sample Return Orbiter," AIAA-2000-4116, AIAA Atmospheric Flight Mechanics Conference, Denver, CO, Aug. 2000.

[5] Rousseau, S.; Perot, E.; Masciarelli, J.; Graves, C.; Queen, E.; "Aerocapture Guidance Algorithm Comparison Campaign for the Mars Premier Mission," AIAA-2002-4822, AIAA/AAS Astrodynamics Specialist Conference, Monterey, CA, August 2002

[6] Masciarelli, J.; Queen, E.; "Guidance Algorithms for Aerocapture at Titan," AIAA-2003-4804, AIAA/ASME/SAE/ASEE Joint Propulsion Conference, Huntsville, AL, July 2003.

[7] Way, D.; Powell R.; Edquist, K.; Masciarelli, J.; Starr, B.; "Aerocapture Simulation and Performance for the Titan Explorer Mission," AIAA 2003-4951, AIAA/ASME/SAE/ASEE Joint Propulsion Conference, Huntsville, AL, July 2003.

[8] Hanak, H.; Crain, T.; Masciarelli, J.; "Revised Algorithm for Analytic Predictor-Corrector Aerocapture Guidance: Exit Phase," AIAA-2003-5746, AIAA Guidance, Navigation, and Control Conference and Exhibit, Austin, TX, August 2003.

[9] Masciarelli, J.; Westhelle, C.; Graves, C.; "Aerocapture Guidance Performance for the Neptune Orbiter," AIAA-2004-4954, AIAA Atmospheric Flight Mechanics Conference and Exhibit, Providence, RI, August 2004.

[10] Starr, B.; Powell, R.; Westhelle, C.; Masciarelli, J.; "Aerocapture Performance Analysis for a Neptune-Triton Exploration Mission," AIAA-2004-4955, AIAA Atmospheric Flight Mechanics Conference and Exhibit, Providence, RI, August 2004.

[11] Starr, B.; Westhelle, C.; "Aerocapture Performance Analysis of a Venus Explorer Mission," AIAA-2005-5913, AIAA Atmospheric Flight Mechanics Conference and Exhibit, San Francisco, California, August 2005.

[12] Masciarelli, J.; "Aerocapture Guidance Algorithm Development and Testing," presented at the NASA Science Technology Conference, College Park, MD, June 2007.

[13] Andrew Keys, A.; Hall, J.; Oh, D.; Munk, M.; "Overview of a Proposed Flight Validation of Aerocapture System Technology for Planetary Missions," AIAA-2006-4518, 42nd AIAA/ASME/SAE/ASEE Joint Propulsion Conference and Exhibit, Sacramento, CA, July 9-12, 2006.

[14] C.G. Justus; F.W. Leslie, "The NASA MSFC Earth Global Reference Atmospheric Model—2007 Version," NASA/TM—2008–215581, November, 2008.